Pergamon

Int. J. Heat Mass Transfer. Vol. 37, No. 18, pp. 2917–2924, 1994

0017–9310/94 $7.00+0.00

0017–9310(94)00122–7

Theory and modeling of phase change materials with and without mushy regions

PETER W. EGOLF and HEINRICH MANZ

Swiss Federal Laboratories for Materials Testing and Research, Ueberlandstrasse 129, CH-8600 Dübendorf, Switzerland

(*Received* 29 *October* 1993 *and in final form* 21 *March* 1994)

Abstract—The continuous-properties model has been developed to numerically solve problems of melting and solidification of substances with a mushy region. The new method is applicable to negligibly small mushy regions. Therefore, it can also be used to numerically calculate the behaviour of materials showing a discontinuous (first-order) phase transition. A stress number, comparable to the Reynolds number of fluid flow, can be introduced to quantify the difficulty of the computational task.

. INTRODUCTION

Melting and solidification occur in many environmental and technical processes. A unique mathematical formulation for the macroscopic phenomenon is called the Stefan problem, after J. Stefan, who was preoccupied with the solidification of water in the polar sea at the end of the last century [1]. Neumann [2] found an analytical solution of the problem in the case of an isothermal semi-infinite domain and a discontinuous temperature change at its boundary. Enormous efforts have been made to solve the Stefan problem by approximate analytical solutions. Several methods, like coordinate transformation, scaling techniques, reduction to integral equations, etc., have been applied [3]. In many practical cases, e.g. in solar engineering, the boundary conditions are stochastic or chaotic, and, therefore, during the last decade an increasing number of applications of numerical methods have been performed. Good results have usually been obtained when an enthalpy formulation was applied (e.g. see refs. [4, 5]).

2. THE BASIC IDEA OF THE MODEL

Several mixtures and glassy substances show a continuous enthalpy transition as a function of temperature from a pure solid to a pure liquid phase. Our idea was to develop a model to calculate the behaviour of only such substances. Taking existing theoretical treatments into consideration, the enthalpy model and the overall specific heat method [6] prove to be very appropriate calculation schemes. The newly developed method is a combination and an extension of these two methods. As we will see in the Section 3, it can also be used to numerically solve the melting and solidification problem of substances without a mushy region. It leads to a nonlinear diffusion equation with a temperature-dependent diffusivity. Therefore, our problem has analogies in moisture transport, in the continuum limit of diffusion-governed chemical reaction kinetics, and in fluid dynamics, and, in general, is described by the shock theory. Different from solutions of Burger's equation—where increasing steepness is driven by a gradient—in our case front creation occurs with a dependence on curvature.

At present the model does not refer to supercooling and natural convection in the liquid phase. As a further simplifying assumption we do not take radiation energy transport in the bulk of the phase change material (PCM) into consideration, because many substances are nearly opaque for black-body radiation in the temperature range of their application. The model can be applied to any (also stochastic or chaotic) initial values and boundary conditions. If alternate heating and cooling occurs, it allows several solid and liquid domains to build up.

Every generalization of the Stefan problem to a storage application will be called a Stefan model (e.g. a two-dimensional approach to a store with a heat transfer fluid). Table 1 shows differences between the Stefan model and the continuous-properties model. As will be shown in Section 5, a larger melting regime corresponds to a weaker nonlinearity of the problem. Therefore, solving the Stefan problem for materials with mushy regions is quite inappropriate. However, the continuous-properties model can be applied to nearly every substance, because in a certain sense it is a generalization of the Stefan model [7].

3. MATHEMATICAL MODELING

As already mentioned, the aim was to construct a model where the continuous transitions of all the physical properties between the two phases, solid and liquid (as a function of temperature), are taken advantage of. If energy conservation is formulated—includ-

NOMENCLATURE

c_p	specific heat	v	velocity
h	specific enthalpy	x	space co-ordinate.
k	thermal conductivity		
s	location of the boundary	Greek symbols	
Sn	new defined stress number for the thermal system	α	thermal diffusivity
		λ	parameter, calculated from equation (35)
Ste	Stefan number	ρ	density
t	time	τ	width of the melting regime (temperature difference).
T	temperature		
$\langle T \rangle$	mean value of a temperature oscillation (temperature level)	Indices	
		1	solid phase
T_f	final temperature	2	liquid phase
T_i	inital temperature	*	modified values (see definition in text).
T_m	(mean) melting temperature		

ing the Fourier law for the heat flux density—we obtain

$$\rho \cdot \frac{\partial h}{\partial t} + \frac{\partial}{\partial x}\left(-k\frac{\partial T}{\partial x}\right) = 0. \tag{1}$$

The heat conductivity k is also a temperature-dependent property. In Section 4 we will give more information on these properties and their nonlinearities. After performing an inner derivative and applying the product law of differential calculus, the result is

$$\rho \cdot \frac{\mathrm{d}h}{\mathrm{d}T} \cdot \frac{\partial T}{\partial t} - k \cdot \frac{\partial^2 T}{\partial x^2} - \frac{\partial k}{\partial x} \cdot \frac{\partial T}{\partial x} = 0. \tag{2}$$

For the whole temperature range the overall specific heat is defined as a derivative of the specific enthalpy:

$$c_p = \frac{\mathrm{d}h}{\mathrm{d}T} \quad h = \int_0^T c_p(T')\,\mathrm{d}T'. \tag{3}$$

The thermal diffusivity is

$$\alpha(T) = \frac{1}{\rho} \cdot \frac{k(T)}{c_p(T)} \tag{4}$$

where we have assumed a constant density ρ. With equations (3) and (4) we obtain

$$\frac{\partial T}{\partial t} = \alpha(T)\left[\frac{\partial^2 T}{\partial x^2} + \frac{1}{k}\frac{\mathrm{d}k}{\mathrm{d}T}\left(\frac{\partial T}{\partial x}\right)^2\right] \tag{5}$$

and

$$\frac{\partial T}{\partial t} = a(T) \cdot \frac{\partial^2 T}{\partial x^2} + b(T) \cdot \left(\frac{\partial T}{\partial x}\right)^2 \tag{6}$$

respectively, with the temperature-dependent coefficients

$$a(T) = \alpha(T) \quad b(T) = \alpha(T) \cdot \frac{1}{k} \cdot \frac{\mathrm{d}k}{\mathrm{d}T}. \tag{7}$$

In chemistry, in the case of constant coefficients a and

Table. 1. Comparison of some features of the Stefan model with those of the continuous-properties model

Effect	Stefan model	Continuous-properties model
Change of physical properties	Discontinuous	Continuous
Interface	Width is zero	Mushy region with finite width unequal to zero
Temperature profile	Discontinuous derivative at the interface location	Is a smooth function
Basic equations	Heat conduction equation for each phase and interface (boundary) condition	Only one nonlinear heat conduction equation with coefficients dependent on temperature
Analytical solutions	Neumann solution	No analytical solutions are known
Degree of nonlinearity	Infinite	Finite
Calculation of the behavior of the following materials is possible:	Exactly: pure materials and crystals	Exact solutions for glasses and mixtures
	Approximately: glassy materials and mixtures	Good numerical solutions for all substances (macroscopic description for engineering purposes)

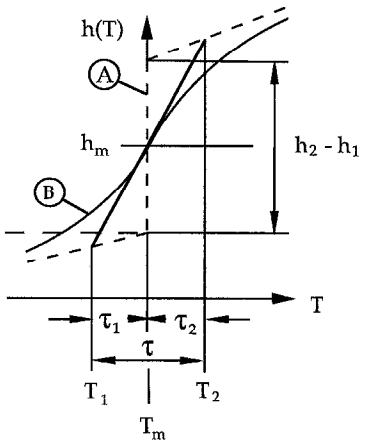

Fig. 1. Discontinuous (dotted line A) and continuous (solid line B) specific enthalpy functions.

b this type of equation is known as a phase diffusion equation [8, 9]:

$$\frac{\partial \Psi}{\partial t} = a \cdot \frac{\partial^2 \Psi}{\partial x^2} + b \cdot \left(\frac{\partial \Psi}{\partial x}\right)^2. \tag{8}$$

Because of the square product of the spatial derivative this equation is nonlinear even when the coefficients considered are constant. It describes chemical reaction front propagations in diffusion-limited reaction diffusion systems. Another important analogy occurs with phenomena in fluid dynamics. Using the Cole–Hopf transformation

$$v = -2 \cdot b \cdot \frac{\partial \Psi}{\partial x} \tag{9}$$

Burger's equation is obtained from relation (8) (see ref. [10]):

$$\frac{\partial v}{\partial t} = a \cdot \frac{\partial^2 v}{\partial x^2} - v \cdot \frac{\partial v}{\partial x} \tag{10}$$

which is known to have a family of shock solutions. In Section 5 it will be shown that in PCM storage devices—analogous to the increasing inclination of fluid dynamical waves—an increase in the inclination of temperature distributions can be observed. In the special case considered here [equation (8) with constant coefficients] a linear relation between the shock front position and time can be derived. In the more general case of temperature-dependent coefficients, as in the description of PCMs with the continuous-properties model, other dependencies—as for example a square root function—can result (e.g. see Fig. 8).

4. CONTINUOUS PROPERTIES OF PCMS

Pure crystalline substances and eutectics show discontinuous enthalpy as a function of temperature. The melting temperature has a sharply defined value T_m (dotted curve A in Fig. 1). Because of a discontinuity the enthalpy is not a unique function of temperature. On the other hand the enthalpy of a mixture or a glassy substance increases, following a smooth curve from the perceived linear behaviour of the solid phase, with gradient c_{p_1}, towards the liquid phase, also with a linear dependence on the slope, c_{p_2} (solid line B in Fig. 1).

Materials with continuous properties as functions of temperature also show continuous behaviour in space. Therefore, between the liquid and the solid, a mushy region—with a width dependent on the physical properties and the dynamics of the system—is observed. To describe the physical properties of a substance, in agreement with the Ginzburg–Landau theory of phase transitions, it would be appropriate to apply polynomial fitting curves. The solid and liquid phases would then each be separated from the mushy region by a critical temperature. As will be seen, from a numerical point of view, it is useful to choose an appropriate analytic function. For example, in the present version of the model the following exponential description has been incorporated:

$$h(T) = c_{p_1} \cdot T + \eta_1: \quad T \leqslant T_m \tag{11}$$

$$h(T) = c_{p_1} \cdot T_m + (h_2 - h_1) + c_{p_2} \cdot (T - T_m) - \eta_2: \quad T > T_m \tag{12}$$

$$\eta_{1,2} = \frac{h_2 - h_1}{2} \cdot \exp\left(-\frac{|T - T_m|}{\tau_{1,2}}\right). \tag{13}$$

Some quantities for these equations are shown in Fig. 1. The equations are asymptotic functions, having respectively, the following forms:

$$T \to -\infty \Rightarrow h(T) \to c_{p_1} \cdot T \quad \text{from equations (11) and (13)} \tag{14}$$

$$T \to +\infty \Rightarrow h(T) \to c_{p_1} \cdot T_m + (h_2 - h_1) + c_{p_2}(T - T_m) \quad \text{from equations (12) and (13)} \tag{15}$$

$$T \to T_m^{\pm} \Rightarrow h \to c_{p_1} \cdot T_m + \frac{h_2 - h_1}{2} = h(T_m) = h_m \quad \text{from equations (11)–(13).} \tag{16}$$

Requiring a function with a continuous derivative at T_m, we obtain

$$c_{p_2} - c_{p_1} = \frac{h_2 - h_1}{2} \cdot \left(\frac{1}{\tau_1} - \frac{1}{\tau_2}\right). \tag{17}$$

An advantage of this approach is that it is possible to clearly define a melting zone:

$$\tau = \tau_1 + \tau_2. \tag{18}$$

It is clear that, with $\tau \to 0$, the discontinuous case A in Fig. 1 will be approached. A modified Stefan number is now defined from this temperature difference and the difference in the specific heat capacities:

$$Ste^* = \frac{(c_{p_2} - c_{p_1}) \cdot \tau}{h_2 - h_1}. \tag{19}$$

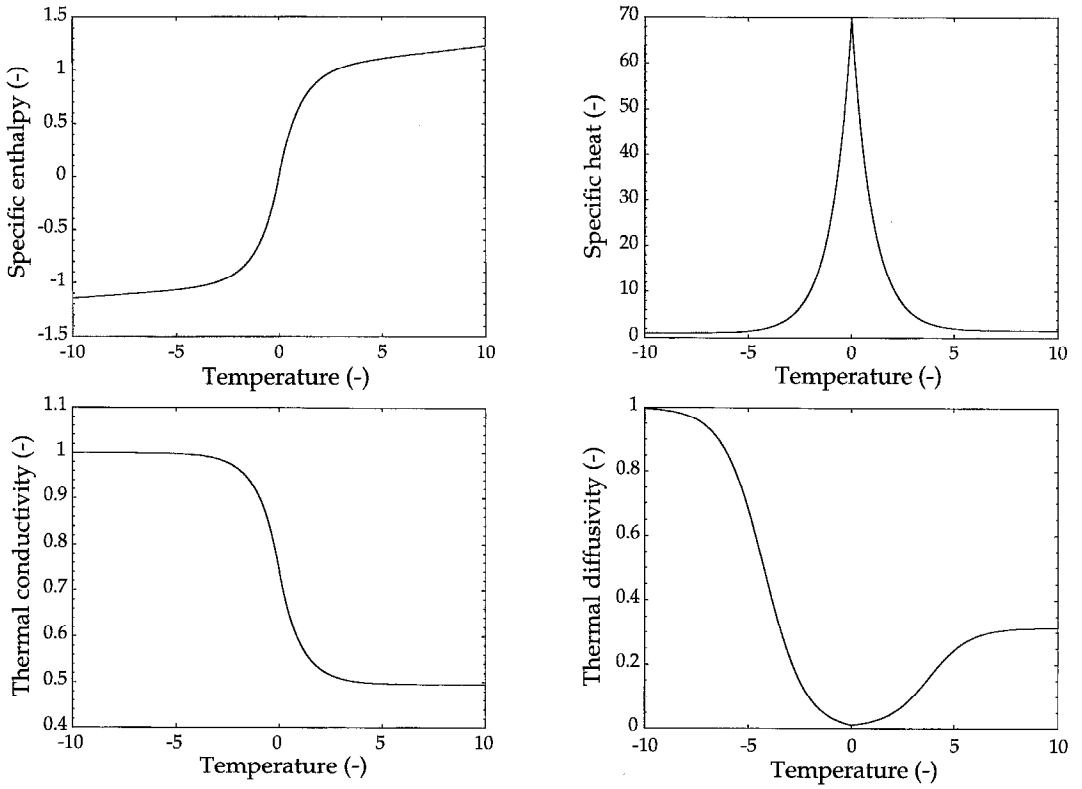

Fig. 2. Four nonlinear physical properties of a PCM.

Assuming τ to be constant, the following quadratic equation can be derived from the last three equations:

$$\tau_1^2 - \left[\left(1+\frac{1}{Ste^*}\right)\cdot\tau\right]\tau_1 + \left(\frac{\tau^2}{2\cdot Ste^*}\right) = 0 \quad (20)$$

which, together with equation (18), leads to two physically relevant solutions:

$$\tau_1 = \frac{1}{2\cdot Ste^*}\left(1+Ste^* - \sqrt{1+(Ste^*)^2}\right)\cdot\tau$$

$$\tau_2 = \frac{1}{2\cdot Ste^*}\left(Ste^* - 1 + \sqrt{1+(Ste^*)^2}\right)\cdot\tau. \quad (21)$$

In the given limits there are the following results:

$$Ste^* \to 0 \Rightarrow \tau_1 \to \tfrac{1}{2}\tau \quad \tau_2 \to \tfrac{1}{2}\tau \quad \text{and}$$

$$Ste^* \to \infty \Rightarrow \tau_1 \to 0 \quad \tau_2 \to \tau. \quad (22)$$

The thermal conductivity has been described by an analogous exponential description, with corresponding widths τ_1 and τ_2 of the mushy region, varying continuously between the constant thermal conductivities k_1 and k_2.

Figure 2 shows four nonlinear properties of a commercially available salt hydrate PCM, based on $CaCl_2 \cdot 6H_2O$. The physical properties have been taken from ref. [11] and the width τ of the melting regime was chosen to be 2 K. They all are constant or linear in the solid domain on the left and in the liquid region at high temperatures. Between the two phases they vary smoothly from one linear regime to the other. Furthermore, the thermal diffusivity also shows constant values in the pure phases and decreases by up to two orders of magnitude towards the mean melting temperature T_m in the mushy region. For all temperatures the density has been assumed constant, equal to the density of the liquid phase:

$$\rho(T) = \rho_2 = \text{constant}. \quad (23)$$

This makes the calculations considerably less difficult. Equation (23) is a first approximation for substances which solidify with small regularly distributed voids inside the solid. A further simplifying assumption is that these cavities do not affect the thermal conductivity noticeably.

In Fig. 2 the quantities have been scaled in the following way:

$$\tilde{T} = \frac{T-T_m}{\left(\frac{\tau}{2}\right)} \quad \tilde{h} = \frac{h-h_m}{\left(\frac{h_2-h_1}{2}\right)} \quad \tilde{\chi} = \frac{\chi}{\chi_1} \quad \chi \in \{k, c_p, \alpha\}. \quad (24)$$

Combining equations (11)–(13), the corresponding description of the thermal conductivity, and formula (3) for the specific heat, and applying the results to equations (4) and (7), one obtains the coefficients $a(T)$

and $b(T)$ of the nonlinear thermal heat equation (6).

5. STRESS NUMBER OF THE THERMAL SYSTEM

To outline some ideas as to how to quantify the nonlinearity of a thermal problem under consideration, we focus on the following special case:

$$\frac{\tau \cdot k}{\Delta k \cdot \Delta T} \gg 1. \tag{25}$$

The following nonlinear diffusion equation is then obtained:

$$\frac{\partial T}{\partial t} = \alpha(T) \cdot \left(\frac{\partial^2 T}{\partial x^2}\right). \tag{26}$$

Now, we expand the thermal diffusivity into a constant term which describes the usual linear diffusion and a nonlinear contribution that is responsible for steepening processes, driven by curvature:

$$\frac{\partial T}{\partial t} = \alpha(T_0) \cdot \frac{\partial^2 T}{\partial x^2} + \Delta\alpha \cdot \frac{\partial^2 T}{\partial x^2} = \alpha_0 \cdot \frac{\partial^2 T}{\partial x^2} + \left.\frac{\mathrm{d}\alpha}{\mathrm{d}T}\right|_{T_0} \cdot (T - T_0) \cdot \frac{\partial^2 T}{\partial x^2} + \ldots \tag{27}$$

The expansion leads to the possibility of defining a stress number Sn for the thermal system:

$$Sn = \frac{\Delta\alpha^*}{\alpha_0} \approx \left\{ \frac{\left.\frac{\mathrm{d}\alpha}{\mathrm{d}T}\right|_{T_0} \cdot \Delta T^*}{\alpha_0} \right\}$$

$$\Delta T^* = \max_{\{T \mid T \in f(T)\}} \{T - T_0\}$$

$$\Delta\alpha^* = \alpha(T_0 + \Delta T^*) - \alpha(T_0). \tag{28}$$

An approximation to the derivative in equation (28) is $\Delta\alpha_{\max}/\tau$ and, therefore, a dimensional analytic estimation of the stress number is

$$Sn = \frac{\Delta\alpha_{\max} \cdot \Delta T^*}{\alpha_0 \cdot \tau}. \tag{29}$$

The number Sn is a measure of the nonlinearity of the thermal phenomena under consideration, comparable with the Reynolds number of fluid flow. If a temperature signal in a PCM occurs at low (or high) temperatures, equation (6) becomes identical to the linear heat conduction equation of the pure solid (or pure liquid) phase:

$$\Delta\alpha^* = 0 \Rightarrow Sn = 0 \Rightarrow \alpha_i = a = \text{constant}$$

$$b = 0 \Rightarrow \frac{\partial T}{\partial t} = \alpha_i \frac{\partial^2 T}{\partial x^2} \quad i \in \{1, 2\}. \tag{30}$$

A high stress number occurs if [see estimation (29)]

$$\tau \to 0 \Rightarrow Sn \to \infty. \tag{31}$$

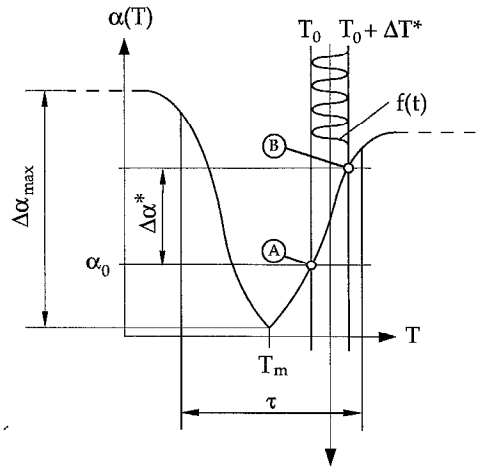

Fig. 3. A sinusoidal temperature signal in the nonlinear thermal diffusivity domain becomes distorted, because different diffusivities occur at different temperatures. Because of an unsteady derivative of the specific heat at the mean temperature T_m (see Fig. 2) the thermal diffusivity, which contains the specific heat in its denominator, gives a kink at this temperature.

Concerning the nonlinearity of a problem, the discontinuous case is the worst kind. It is well known that in a linear case temperature distributions are at most damped and phase-shifted. On the other hand, when a signal is located in the vicinity of the melting temperature T_m the temperature perturbation becomes distorted because different diffusivities occur at different temperatures. In Fig. 3 a sinusoidal perturbation has differences in its diffusivity up to $\Delta\alpha^*$ [compare the values at the minimum (A) and the maximum (B)]. Looking at Fig. 3 it is possible to give physical explanations for each of the steepening processes that occur. The sign of the product of the difference in diffusivity and the curvature of the temperature profile is important, and is proportional to the second spatial derivative. For oscillatory temperature distributions at different mean temperatures $\langle T \rangle$ and for corresponding local minima and maxima, the signs are given in Table 2 (case 1 is shown in Fig. 3). If the product $\Delta\alpha^* \cdot \kappa$ is positive, then the nonlinear contribution, represented by the second term on the right-hand side of equation (27), gives a positive contribution to the time derivative of the temperature. Therefore, the nonlinear perturbation increases in the positive time direction and a steepening process on the right-hand side (front) of the profile will occur (see encircled number one in Fig. 4). If the entire temperature distribution is taken into consideration, this phenomenon causes a slowing down of the diffusion process at the front; but this also increases its inclination. From equation (27) we conclude that nonlinear diffusion can be regarded as the occurrence of the usual linear diffusion with the superposition of nonlinear forward or backward steepening. To illustrate the results of Table 2, we have performed some numerical calculations, presented in Fig. 4. Numbers

Table. 2. Signs of the diffusivity difference and curvature of the temperature distribution determining the direction of increasing steepness.

Case	Difference in diffusivity $\Delta\alpha^*$	Curvature κ	$\Delta\alpha^* \cdot \kappa$	Increasing steepness to the:
1	>0	<0	<0	Back (left)
2	>0	>0	>0	Front (right)
3	<0	<0	>0	Front (right)
4	<0	>0	<0	Back (left)

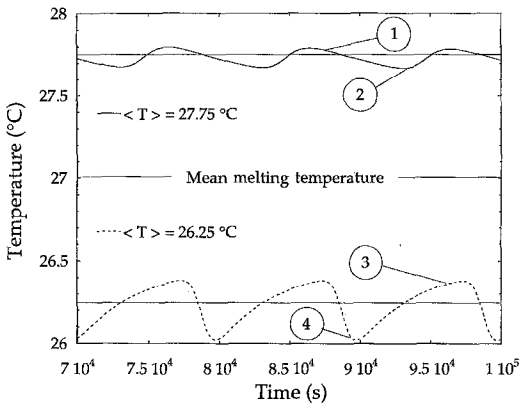

Fig. 4. Forward and backward steepening of temperature functions with mean temperatures $\langle T \rangle$ above and beneath the mean melting temperature $T_m = 27°C$. The encircled numbers indicate the four different cases presented in Table 2.

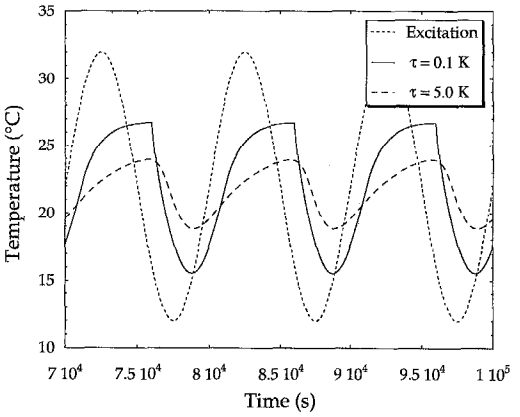

Fig. 5. Steepening in the melting region. A smaller width of the melting region leads to a more intense steepening of the temperature distribution. The mean temperature is $\langle T \rangle = 22°C$.

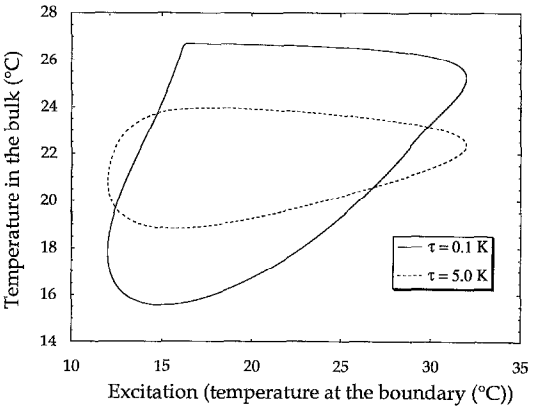

Fig. 6. Phase portrait representation of the periodic steady-state solutions shown in Fig. 5.

1–4 correspond to the four different cases given in Table 2.

The calculations were performed for a one-dimensional slab of 10 cm thickness. The temperature was calculated for a depth of 2.5 cm from a surface. The excitations had an amplitude of 2 K and the period was 10 000 s. They were applied with equal phases to the boundaries on each side of the slab. Because of the small excitation amplitudes and mean temperatures $\langle T \rangle$ quite close to the mean melting temperature T_m, we could also obtain steepening at the extremes of temperature oscillation more distant from T_m.

The intensity of a steepening process increases with decreasing width of the melting regime. This can clearly be seen in Fig. 5, where calculations are presented for two different widths, 5 and 0.1 K. The excitation at the boundary is also shown (dotted line). In contrast to the examples in Fig. 4, the excitation amplitude has a higher value of 10 K. Therefore, the temperatures at the minima reach down into the pure solid phase at 19°C ($\tau = 5$ K) and 16°C ($\tau = 0.1$ K), respectively. At these temperatures usual linear diffusion without steepening occurs. That is the reason why the temperature distribution keeps its sinusoidal shape in the vicinity of the local minima. Figure 6 shows a phase space representation of the same temperature oscillations. We note that all these solutions are steady periodic oscillations, occurring after a relaxation time of 19.4 h.

6. PERFORMANCE OF THE MODEL

In order to test the new model, we have chosen Neumann's analytical solution, which describes discontinuous front propagation. An infinite half plane is initially at a constant temperature T_i above the melting temperature T_m. At time $t = 0$ the boundary temperature is lowered to T_f below T_m. For this case

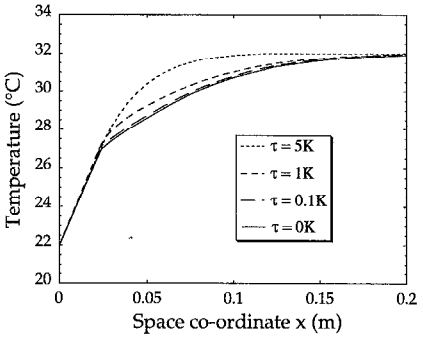

Fig. 7. Temperature distributions for different widths of the melting region. The discontinuous phase boundary can be identified by finding a kink in the Neumann solution ($\tau = 0$): after 5 h freezing time it is located at 2.35 cm.

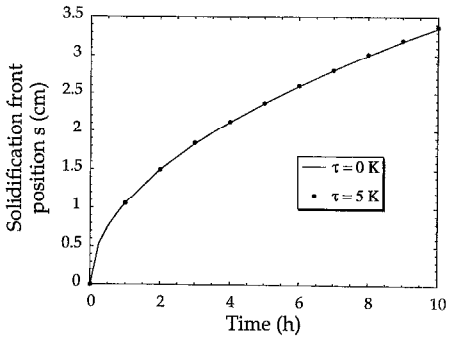

Fig. 8. Solidification front position as a function of time.

the solution of the Stefan problem, discussed in Section 2 is [11]

$$\frac{T_1 - T_f}{T_m - T_f} = \frac{\operatorname{erf}\left(\dfrac{x}{2 \cdot \sqrt{\alpha_1 \cdot t}}\right)}{\operatorname{erf}(\lambda)}: \quad 0 < x \leqslant s(t) \quad (32)$$

$$\frac{T_i - T_2}{T_i - T_m} = \frac{\operatorname{erfc}\left(\dfrac{x}{2 \cdot \sqrt{\alpha_2 \cdot t}}\right)}{\operatorname{erfc}\left(\lambda \cdot \sqrt{\dfrac{\alpha_1}{\alpha_2}}\right)}: \quad s(t) < x \quad (33)$$

with the phase boundary located at

$$s(t) = 2 \cdot \lambda \cdot \sqrt{\alpha_1 \cdot t}. \quad (34)$$

A transcendental equation is obtained by substituting these solutions into the phase boundary condition of the Stefan problem [11]:

$$\frac{Ste}{\sqrt{\pi} \cdot \lambda} \cdot \left[\frac{\exp(-\lambda^2)}{\operatorname{erf}(\lambda)} - \frac{\beta' \cdot \gamma'}{\alpha'^2} \cdot \frac{\exp(-\beta'^2 \cdot \lambda^2)}{\operatorname{erfc}(\beta' \cdot \lambda)} \right] = 1. \quad (35)$$

The following abbreviations have been introduced:

$$Ste = \frac{c_{p_1} \cdot (T_m - T_f)}{h_2 - h_1} \qquad \alpha' = \sqrt{\frac{k_1}{k_2}}$$

$$\beta' = \sqrt{\frac{\alpha_1}{\alpha_2}} \qquad \gamma' = \frac{T_i - T_m}{T_m - T_f}. \quad (36)$$

Solving equation (35) determines the parameter λ, which has to be known to plot the analytical solutions (32)–(34). In Fig. 7 numerical solutions—with different τs—are shown together with the Neumann solution ($\tau = 0$). For a decreasing τ the temperature curves show an increasing curvature at the position of the solidification front and approach the Neumann solution for τ tending to zero. Figure 8 illustrates that—in this example—we could not find any significant deviations in the positions of the fronts, comparing cases with small and large mushy regions, for quite a large time interval of 10 h.

All the results presented were obtained with an ordinary finite-difference scheme. It is astonishing how well the continuous-properties model applies even to melting zone widths of only small fractions of 1 K (e.g. 1/100 K). Therefore, we conclude that the model can also be used to numerically calculate melting and solidification of materials without mushy regions with high precision.

For the finite-difference scheme the Courant–Friedrichs–Lewy stability criterion exists that is sufficient but not necessary [12]. For nonlinear diffusivities this criterion has to be modified (see ref. [13]). It is seen that a nonconstant steep diffusivity function and the high dimensionality of the problem demand small time steps.

7. CONCLUSIONS AND OUTLOOK

We have presented a theory and some first calculations concerning a new model that initially has been developed to calculate melting and solidification of materials with mushy regions. The possibility to numerically solve problems with very thin mushy domains makes the model, for practical purposes, also apply correctly to substances with discontinuous phase boundaries. At present, we are studying how successfully it can be applied to PCMs, for example salt hydrates, which we intend to use for solar engineering applications. First investigations of the behaviour of a two-dimensional store, with air acting as the heat transport fluid, show a good agreement between experimental results and solutions of numerical simulations.

Acknowledgements—The financial assistance of the National Energy Research Fund (NEFF) and the support of B. Barp, J. Brun, H. Gränicher and M. Zimmermann are thankfully acknowledged.

REFERENCES

1. J. Stefan, Ueber die Theorie der Eisbildung, insbesondere über die Eisbildung im Polarmeer, *Annln Phys. Chem.* **42,** 269–286 (1891).
2. F. Neumann, In *Die partiellen Differentialgleichungen der Physik*, Vol. 2, p. 117. B. Riemann, H. Weber, F. Vieweg, Braunschweig (1912).
3. J. Crank, *Free and Moving Boundary Problems*, p. 114. Clarendon Press, Oxford (1984).
4. W. J. Minkowycz, E. M. Sparrow, G. E. Schneider and R. H. Pletcher, *Handbook of Numerical Heat Transfer*, p. 747. John Wiley, New York (1988).
5. V. R. Voller, Fast implicit finite-difference method for the analysis of phase change problems, *Numer. Heat Transfer* **17B,** 155–169 (1990).
6. M. Nishimura, Y. Bando, M. Kuraishi and E. W. P. Hahne, Direct solar thermal energy storage using a semi-transparent PCM, *Kagaku Kogaku Ronbunshu* **13,** 435–441 (1987).
7. A. Bossavit, A. Damlamian and M. Fremond, *Free Boundary Problems: Applications and Theory*, Vol. 3, p. 1. Pitman Advanced Publishing Program (1985).
8. Y. Kuramoto, *Chemical Oscillations, Waves and Turbulence*, p. 89. Springer-Verlag, Berlin (1984).
9. L. Galfi and Z. Rácz, Properties of the reaction front in an $A+B \rightarrow C$ type reaction diffusion process, *Phys. Rev. A* **38,** 3151–3154 (1988).
10. G. B. Witham, *Linear and Nonlinear Waves*, Pure and Applied Mathematics, p. 96. Wiley–Interscience Series of Texts, Monographs and Tracts (1974).
11. G. A. Lane, *Solar Heat Storage: Latent Heat Materials*, Vol. 2, p. 16. CRC Press, Boca Raton, FL (1983).
12. H. S. Carslaw and J. C. Jaeger, *Conduction of Heat in Solids* (2nd Edn), p. 471. Clarendon Press, Oxford (1959).
13. P. W. Egolf and P. Steiner, Two-dimensional moisture transfer in a lime–sand stone specimen, nonlinear diffusion, International Energy Agency, report T1-CH-93/01 (April 1993) (can be ordered from the authors).